

Human-Machine Shared Control Approach for the Takeover of Cooperative Adaptive Cruise Control

Haoran Wang, *Member, IEEE*, Zhenning Li, Arno Eichberger, Jia Hu, *Senior Member, IEEE*

Abstract—Cooperative Adaptive Cruise Control (CACC) often requires human takeover for tasks such as exiting a freeway. Direct human takeover can pose significant risks, especially given the close-following strategy employed by CACC, which might cause drivers to feel unsafe and execute hard braking, potentially leading to collisions. This research aims to develop a CACC takeover controller that ensures a smooth transition from automated to human control. The proposed CACC takeover maneuver employs an indirect human-machine shared control approach, modeled as a Stackelberg competition where the machine acts as the leader and the human as the follower. The machine guides the human to respond in a manner that aligns with the machine's expectations, aiding in maintaining following stability. Additionally, the human reaction function is integrated into the machine's predictive control system, moving beyond a simple "prediction-planning" pipeline to enhance planning optimality. The controller has been verified to i) enable a smooth takeover maneuver of CACC; ii) ensure string stability within a specific Operational Design Domain (ODD) when human control authority is below 32.7%; iii) enhance both perceived and actual safety through machine interventions; and iv) reduce the impact on upstream traffic by up to 60%.

Index Terms—CACC, Platoon takeover, human-machine shared control, game-based model predictive control

I. INTRODUCTION

Cooperative Adaptive Cruise Control (CACC) is deemed to be a promising technology in the field of cooperative automation. By enabling conventional Adaptive Cruise Control (ACC) with communication and cooperation, CACC is capable of maneuvering Cooperative and Autonomous Vehicles (CAVs) tightly following the preceding vehicle. CACC has been verified to double road capacity [1-3], save 10%-20% of energy [4], and reduce 14% of carbon dioxide emission [5].

Although bearing these merits, CACC is not yet widely

promoted in field implementations. One of the main concerns is the safety risks during the takeover maneuver. In the field implementation of CACC, a human driver would take over the control authority from time to time, including conducting a lane change and exiting a highway. Great risks arise if the driver directly takes over the control authority. This argument stands on the different characteristics of human driving compared to CACC. First, the close-following strategy of CACC increases collision risks when taken over by a human [6]. According to field tests, the following headway in a CACC platoon could be reduced to 0.5 seconds, much shorter than the 1-2 seconds headway of the conventional ACC and Human-driven Vehicle (HV) [7]. The close-following strategy of CACC is usually perceived as unsafe for a human driver. Suffering this unsafe feeling, the human driver tends to conduct hard braking without the consideration of his back. The human driver's stress behavior would cause collisions. Second, a human driver is physiologically unable to get into a groove quickly [8]. Past studies indicate that a human takes 7-9 seconds to regain his driving ability [9]. The driver may not react timely to emergencies during a takeover maneuver. Therefore, it is quite crucial to ensure the safety of CACC's takeover.

However, as far as we know, there are still no studies developing takeover controllers for CACC. Past studies mostly focus on the regular operation of CACC [10-14]. However, in takeover maneuvers, these CACC controllers are not compatible anymore. A coexistent strategy for both human and machine shall be developed. A smooth control authority transition from machine to human shall be realized. Nevertheless, previous studies have proposed various methods for the takeover of other systems [15-18]. These studies would provide great inspiration for the takeover of CACC systems.

In recent years, human-machine shared control has been a hot topic in the field of automated driving [19, 20]. The human-machine shared control method can be typically divided into two categories: direct shared control and indirect shared control

*This paper is partially supported by National Key R&D Program of China (2022YFF0604905), National Natural Science Foundation of China (Grant No. 52302412 and 52372317), Yangtze River Delta Science and Technology Innovation Joint Force (No. 2023CSJGG0800), the Fundamental Research Funds for the Central Universities, Tongji Zhongte Chair Professor Foundation (No. 000000375-2018082), the Postdoctoral Fellowship Program (Grade B) of China Postdoctoral Science Foundation (GZB20230519), Shanghai Sailing Program (No. 23YF1449600), Shanghai Post-doctoral Excellence Program (No.2022571), China Postdoctoral Science Foundation (No.2022M722405), and the Science Fund of State Key Laboratory of Advanced Design and Manufacturing Technology for Vehicle (No. 32215011). (*Corresponding author: Jia Hu.*)

H. Wang is with Key Laboratory of Road and Traffic Engineering of the Ministry of Education, Tongji University, Shanghai 201804, China, and State

Key Laboratory of Advanced Design and Manufacturing for Vehicle Body, Hunan University, Changsha, 410082, China (e-mail: wang_haoran@tongji.edu.cn).

Z. Li is with State Key Laboratory of Internet of Things for Smart City, Departments of Civil and Environmental Engineering and Computer and Information Science, University of Macau, Avenida da Universidade Taipa, Macau, China. (e-mail: zhenningli@um.edu.mo).

A. Eichberger is with Institute of Automotive Engineering, Graz University of Technology, Graz, A-8010, Austrian. (e-mail: arno.eichberger@tugraz.at).

J. Hu is with Key Laboratory of Road and Traffic Engineering of the Ministry of Education, Tongji University, Shanghai 201804, China. (e-mail: hujia@tongji.edu.cn).

[21]. The direct shared control imposes the machine's commands on the steering wheel via haptic feedback [22, 23]. This type of method cannot be adapted to the CACC takeover scenario, since longitudinal shared control cannot be realized via throttle or brake pedals' direct feedback. To address this challenge, the indirect shared control method is proposed to generate machine inputs and fuse with human commands before execution [24-26].

In this paper, in response to the practical requirement of implementing CACC, this study introduces a novel CACC takeover controller based on the human-machine indirect shared control approach. The proposed controller bears the following contributions:

- **Enabling a smooth takeover maneuver of CACC:** The controller employs a human-machine indirect shared control approach to facilitate a seamless transition from automated to human control. *Machine interventions help mitigate human drivers' aggressive responses*, such as hard braking, which are often triggered by the close-following strategy of CACC. By gradually transferring control authority from the machine to the human, the controller ensures a smooth takeover process.

- **Achieving planning optimality in human-machine shared control:** Unlike the traditional "prediction-planning" pipeline, *this research integrates the human reaction function into the machine's predictive control system*, ensuring planning optimality. The human-machine shared control is modeled as a Stackelberg competition, with the machine's planning framed as a Game-based Model Predictive Control (GMPC) problem. By incorporating the human reaction function into the system dynamics, the machine's commands are derived as optimal solutions considering human reaction rationales.

- **Ensuring string stability within a specific Operational Design Domain (ODD):** The proactive interventions of the machine enable the ego-vehicle to anticipate the actions of the platoon leader by utilizing the future actions of preceding

vehicles. Allocating partial control authority to the machine stabilizes the CACC system, preventing oscillations from propagating along the string. *The ODD for maintaining string stability has been quantified* based on various factors of authority allocation between the human and the machine.

- **Enhancing driving safety and reduced traffic impacts:**

The proposed controller's proactive commands reduce following gap oscillations and acceleration magnitude. Hence, it enhances both perceived safety and actual safety. Additionally, the maintenance of string stability minimizes oscillations experienced by the last CAV in the platoon, thereby mitigating adverse effects on upstream traffic.

II. METHODOLOGY

The proposed CACC takeover controller follows the human-machine shared control framework. In the system, each CAV would make a Stackelberg competition with its human driver. Human reaction function is modeled and considered in the machine's planning. The machine's planned commands are fused with the human driver's commands for execution.

A. System structure

The system structure of the proposed controller is shown in Fig. 1. The CACC platoon follows a Predecessor-Following (PF) topology [27]. CAVs within the platoon are controlled in a distributed approach. Each CAV is under the shared control of human and machine. From the human side, the human driver wants to switch his role from supervising to driving. The human monitors the preceding vehicle and makes throttle or brake commands to approach the desired path. From the machine side, the machine controller obtains status information on the environment via onboard perception and communication. The machine outputs commands to maintain the following stability. Obtaining commands from human and machine, a shared control law is designed to generate final adjusted commands to steer-by-wire chassis.

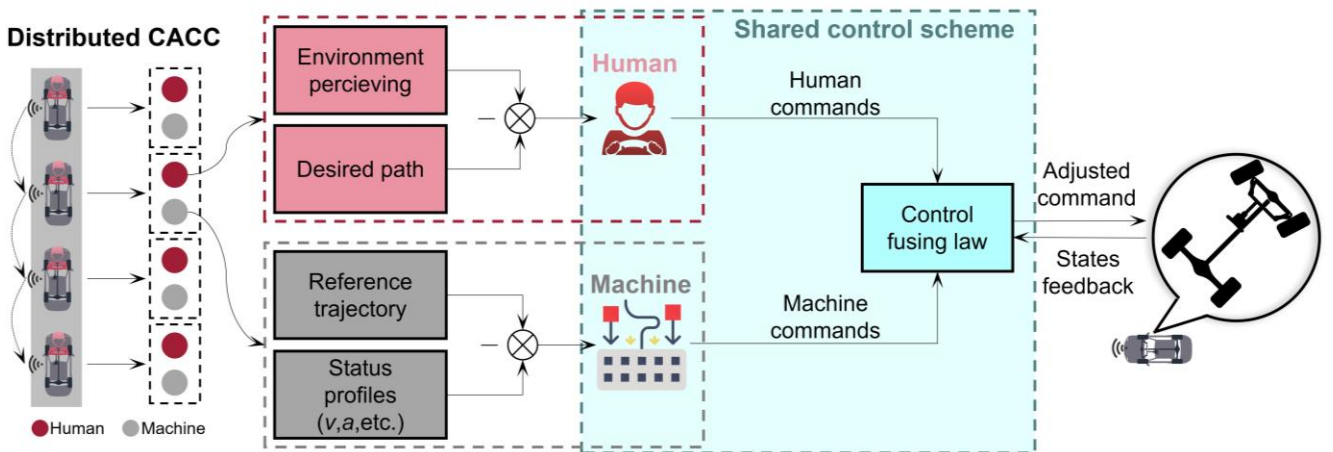


Fig. 1. System framework for CACC takeover

A human and machine indirect shared control scheme [24] is adopted for the takeover maneuver of CACC, as illustrated in

Fig. 2. This scheme mainly consists of three modules: human driver, human modeling, machine controller, and control

fusing.

- **Human driver:** The human driver would manipulate the throttle and brake to control the vehicle. Human commands are transformed into commanded acceleration as the input of control fusing.

- **Human modeling:** A Model Predictive Control (MPC) based modeling method is proposed to model the human's reaction to the environment. The modeling outputs a human reaction function, which reveals the law of human driver's behavior. The human reaction function would be considered in the formulation of human-machine system dynamics in machine planning.

- **Machine controller:** The machine controller is formulated into a GMPC problem. The machine would conduct

a Stackelberg competition with the human. In this competition, machine is the leader, and the human is the follower. The machine is with the objective of leading the human to react as the machine expects. Hence, a human and machine shared system dynamics model is formulated by introducing the human reaction function into the dynamics model. In this way, the machine is capable of leading the human as expected to realize a stable following.

- **Control fusing:** This module is proposed to generate the final commands. A typical control fusing function is adopted. It considers the ODD of ensuring string stability to allocate control authorities between human and machine. Weighting factors are decided to fuse human and machine commands. Final adjusted commands are outputted for local execution.

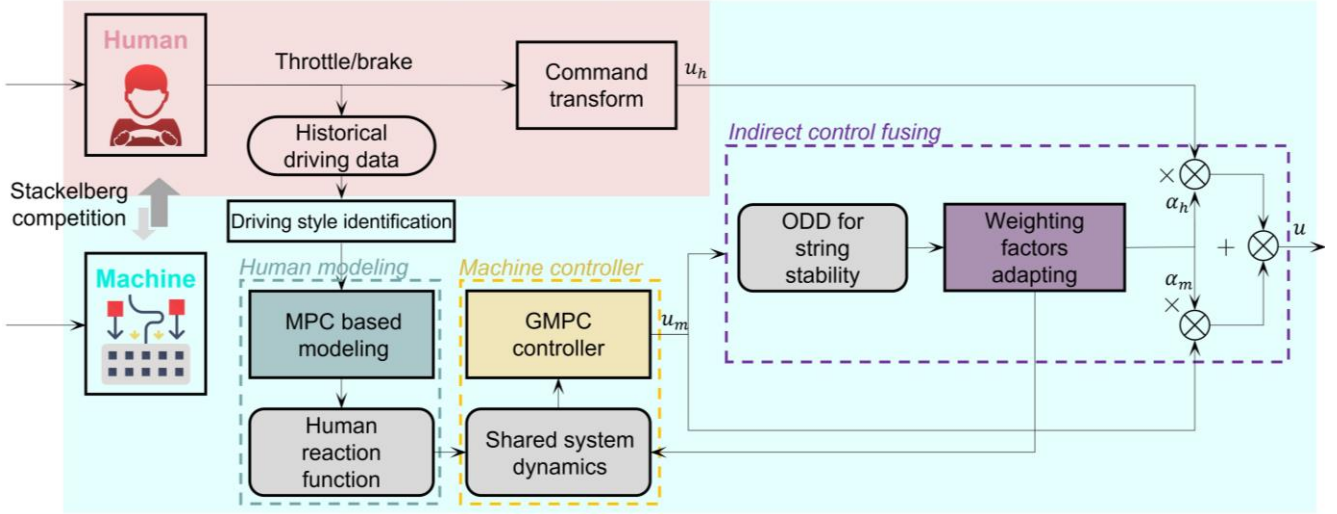


Fig. 2. Stackelberg competition based indirect shared control scheme

B. Definition and Declaration

Following the distributed CACC system structure, each CAV within the platoon is controlled by a human and machine shared controller. Hence, the following formulation only presents a CAV's controller. State and control vectors of a human-machine shared control CAV are defined in the following.

State vector \mathbf{x}_k at control step k is defined as follows.

$$\mathbf{x}_k \stackrel{\text{def}}{=} [\Delta v_k, g_k]^T \quad (1)$$

where Δv_k is the speed difference between ego-CAV and its preceding vehicle; g_k is the following gap between ego-CAV and its preceding vehicle. Δv_k and g_k are defined as follows.

$$\Delta v_k \stackrel{\text{def}}{=} v_k - v_k^p \quad (2)$$

$$g_k \stackrel{\text{def}}{=} x_k^p - x_k \quad (3)$$

where v_k is the speed of ego-CAV; v_k^p is the speed of the preceding vehicle; x_k^p is the longitudinal position of the preceding vehicle; x_k is the longitudinal position of ego-CAV. The preceding vehicle could be an HV or CAV.

The desired state is defined as Eqs. (4) and (5). $\mathbf{x}_{h,k}^{\text{ref}}$ is the desired state of human driver. $\mathbf{x}_{m,k}^{\text{ref}}$ is the desired state of machine controller. When human driver takes over the

authority, it generally expects a greater following gap $g_{h,k}^{\text{ref}}$, and ignores the following stability. The machine controller expects to maintain the stable following status.

$$\mathbf{x}_{h,k}^{\text{ref}} \stackrel{\text{def}}{=} [\sim, g_{h,k}^{\text{ref}}]^T \quad (4)$$

$$\mathbf{x}_{m,k}^{\text{ref}} \stackrel{\text{def}}{=} [0, \sim]^T \quad (5)$$

According to the indirect shared control scheme, the control vector \mathbf{u}_k is the fusion of human's control vector $\mathbf{u}_{h,k}$ and machine's control vector $\mathbf{u}_{m,k}$, as shown in Eq. (6).

$$\mathbf{u}_k \stackrel{\text{def}}{=} \alpha_{h,k} \mathbf{u}_{h,k} + \alpha_{m,k} \mathbf{u}_{m,k} \quad (6)$$

$$\mathbf{u}_{h,k} \stackrel{\text{def}}{=} a_{h,k} \quad (7)$$

$$\mathbf{u}_{m,k} \stackrel{\text{def}}{=} a_{m,k} \quad (8)$$

where $\alpha_{h,k}$ is the authority allocation factor of human's command; $\alpha_{m,k}$ is the authority allocation of machine's command. Typically, $\alpha_{h,k} + \alpha_{m,k} = 1$ to avoid outliers. $a_{h,k}$ is the human's commanded acceleration; $a_{m,k}$ is the machine's commanded acceleration.

C. Human-machine shared system dynamics model

Derivatives of state variables in Eq. (1) are as follows.

$$\frac{d\Delta v(t)}{dt} = a^p(t) - a(t) \quad (9)$$

$$\frac{dg(t)}{dt} = \Delta v(t) \quad (10)$$

where a^p is the speed of the preceding vehicle.

Formulating the Eqs. (9) and (10) into a state-space form as follows [28].

$$\dot{\mathbf{x}}(t) = \mathbf{A}'\mathbf{x}(t) + \mathbf{B}'\mathbf{u}(t) + \mathbf{C}'a^p(t) \quad (11)$$

where $\mathbf{A}' \stackrel{\text{def}}{=} \begin{bmatrix} 0 & 0 \\ 1 & 0 \end{bmatrix}$, $\mathbf{B}' \stackrel{\text{def}}{=} \begin{bmatrix} -1 \\ 0 \end{bmatrix}$, $\mathbf{C}' \stackrel{\text{def}}{=} \begin{bmatrix} 1 \\ 0 \end{bmatrix}$.

The continuous formulation of system dynamics shall be discretized since vehicle control is generally implemented in a discrete domain. Applying the forward Euler method, the control input is assumed to be constant within each update interval Δt : $\mathbf{u}(t) = \mathbf{u}_k$ where k is the control step index and $k\Delta t \leq t < (k+1)\Delta t$. The discretization is close to the original continuous form since the control interval is generally sufficiently small [29]. The continuous system dynamics could then be discretized as follows.

$$\mathbf{x}_{k+1} = \mathbf{A}\mathbf{x}_k + \mathbf{B}_{h,k}\mathbf{u}_{h,k} + \mathbf{B}_{m,k}\mathbf{u}_{m,k} + \mathbf{C}a_k^p, \quad (12)$$

$k \in [0, K)$

where $\mathbf{A} \stackrel{\text{def}}{=} \mathbf{I} + \mathbf{A}'\Delta t$, $\mathbf{B} \stackrel{\text{def}}{=} \mathbf{B}'\Delta t$, $\mathbf{B}_{h,k} \stackrel{\text{def}}{=} \mathbf{B}\alpha_{h,k}$, $\mathbf{B}_{m,k} \stackrel{\text{def}}{=} \mathbf{B}\alpha_{m,k}$, and $\mathbf{C} = \mathbf{C}'\Delta t$. K is the control horizon.

It should be noted that the vehicle state updating rule is different from the view of human and machine. The machine controller is capable of obtaining the future actions of the preceding CAV via communication within the platoon. The human driver can only perceive the current state of the preceding vehicle. Accurate future actions are not available for human. Hence, from the view of human, $\mathbf{C}a_k^p$ is not obtained in the dynamics model (12).

D. Human driving modeling

The human driver makes optimal driving decisions based on the real-time prediction of the surrounding environment. Human's decision-making scheme strongly agrees with the logic of MPC [30]. Hence, an MPC framework is adopted to model human driving in this research. The optimal control law of the MPC problem is the human's reaction function to the environment. Detailed formulation and inference are provided in the following.

1) MPC-based human driving model

The human driving model could be formulated into the form of the LQR problem as follows. It aims at finding the optimal control series $\mathbf{u}_{h,k}|_{k=1}^{k=K}$ to minimize human's objective function J_h .

$$\min_{\mathbf{u}_{h,k}|_{k=1}^{k=K}} (J_h) = \sum_{k=1}^{K-1} \Phi_{h,k}(\mathbf{x}_k, \mathbf{u}_{h,k}, \mathbf{u}_{m,k}, \mathbf{x}_{h,k}^{ref}) + \Psi_{h,K}(\mathbf{x}_K, \mathbf{x}_{h,K}^{ref}) \quad (13)$$

$$\text{s.t. vehicle dynamics: } f_h(\mathbf{x}_k, \mathbf{u}_{h,k}, \mathbf{u}_{m,k}) = 0 \quad (14)$$

where $\Phi_{h,k}$ is the running cost of human driving; $\Psi_{h,K}$ is the terminal cost of human driving; f_h is the vehicle dynamics. The three functions are formulated as follows.

$$\Phi_{h,k} \stackrel{\text{def}}{=} \frac{1}{2}(\mathbf{x}_k - \mathbf{x}_{h,k}^{ref})^T \mathbf{Q}_{h,k}(\mathbf{x}_k - \mathbf{x}_{h,k}^{ref}) + \frac{1}{2}\mathbf{u}_{h,k}^T \mathbf{R}_{h,k}\mathbf{u}_{h,k} \quad (15)$$

$$\Psi_{h,K} \stackrel{\text{def}}{=} \frac{1}{2}(\mathbf{x}_K - \mathbf{x}_{h,K}^{ref})^T \mathbf{Q}_{h,K}(\mathbf{x}_K - \mathbf{x}_{h,K}^{ref}) \quad (16)$$

$$f_h = \mathbf{x}_{k+1} - \mathbf{A}\mathbf{x}_k + \mathbf{B}_{h,k}\mathbf{u}_{h,k} + \mathbf{B}_{m,k}\mathbf{u}_{m,k} \quad (17)$$

where $\mathbf{Q}_{h,k} = \text{diag}[q_{h,k}^v, q_{h,k}^g]$. $q_{h,k}^v$, $q_{h,k}^g$, and $\mathbf{R}_{h,k}$ are weighting factors of speed error cost, gap error cost, and control effort cost, respectively. They are all positive. The vehicle dynamics model is obtained from Eq. (12) after removing the item of the preceding vehicle's future actions $\mathbf{C}a_k^p$.

2) Human reaction function

The human reaction function is the optimal control law of the problem (13). The control law is deduced based on the dynamic programming approach, as shown in [Theorem 1](#).

Theorem 1: The human's action function is as follows.

$$\mathbf{u}_{h,k} = \mathbf{K}_{h,k}\mathbf{x}_k + \mathbf{P}_{h,k}\mathbf{u}_{m,k} + \mathbf{S}_{h,k} \quad (18)$$

where

$$\mathbf{H}_{h,k} \stackrel{\text{def}}{=} (\mathbf{R}_{h,k} + \mathbf{B}_{h,k}^T \mathbf{D}_{k+1} \mathbf{B}_{h,k})^{-1} \quad (19)$$

$$\mathbf{K}_{h,k} \stackrel{\text{def}}{=} -\mathbf{H}_{h,k} \mathbf{B}_{h,k}^T \mathbf{D}_{k+1} \mathbf{A} \quad (20)$$

$$\mathbf{P}_{h,k} \stackrel{\text{def}}{=} -\mathbf{H}_{h,k} \mathbf{B}_{h,k}^T \mathbf{D}_{k+1} \mathbf{B}_{m,k} \quad (21)$$

$$\mathbf{S}_{h,k} \stackrel{\text{def}}{=} -\mathbf{H}_{h,k} \mathbf{B}_{h,k}^T \mathbf{F}_{k+1} \quad (22)$$

$$\mathbf{N}_k \stackrel{\text{def}}{=} \mathbf{A} + \mathbf{B}_{h,k} \mathbf{K}_{h,k} \quad (23)$$

$$\mathbf{M}_{h,k} \stackrel{\text{def}}{=} -(\mathbf{K}_{h,k}^T \mathbf{R}_{h,k} + \mathbf{N}_k^T \mathbf{D}_{k+1} \mathbf{B}_{h,k}) \mathbf{H}_{h,k} \mathbf{B}_{h,k}^T \quad (24)$$

where \mathbf{D}_k , and \mathbf{F}_k are concomitant coefficient matrices that could be computed in reverse order:

$$\mathbf{D}_k = \mathbf{Q}_{h,k} + \mathbf{K}_{h,k}^T \mathbf{R}_{h,k} \mathbf{K}_{h,k} + \mathbf{N}_k^T \mathbf{D}_{k+1} \mathbf{N}_k \quad (25)$$

$$\mathbf{F}_k = -\mathbf{Q}_{h,k} \mathbf{x}_{h,k}^{ref} + (\mathbf{M}_{h,k} + \mathbf{N}_k^T) \mathbf{D}_{k+1} \mathbf{B}_{m,k} \mathbf{u}_{m,k} + (\mathbf{M}_{h,k} + \mathbf{N}_k^T) \mathbf{F}_{k+1} \quad (26)$$

where $\mathbf{D}_K = \mathbf{Q}_{h,K}$ and $\mathbf{F}_K = -\mathbf{Q}_{h,K} \mathbf{x}_{h,K}^{ref}$.

Proof:

Based on the dynamic programming logic, the cost-to-go function of problem (13) is defined as $V(\mathbf{x}_k)$ in Eq. (27) as follows.

$$V(\mathbf{x}_k) = \min_{\mathbf{u}_{h,i}|_{i=k}} \sum_{i=k}^{K-1} \Phi_{h,i} + V(\mathbf{x}_K) \quad (27)$$

$$V(\mathbf{x}_K) = \Psi_{h,K} \quad (28)$$

where $V(\mathbf{x}_k)$ is the cost-to-go function at the step k .

Based on the Bellman's optimality principle, the optimal solution could be obtained by iteratively optimizing $V(\mathbf{x}_k)$ from the step $K-1$ to the step 1. At the step k , the cost-to-go function $V(\mathbf{x}_k)$ is assumed be fit into a second-order form as follows.

$$V(\mathbf{x}_k) = \Phi_{h,k} + \frac{1}{2} \mathbf{x}_{k+1}^T \mathbf{D}_{k+1} \mathbf{x}_{k+1} + \mathbf{x}_{k+1}^T \mathbf{F}_{k+1} + \mathbf{G}_{k+1} \quad (29)$$

where \mathbf{D} , \mathbf{F} , and \mathbf{G} are coefficient matrices that would be inferred in the following.

The derivative of $V(\mathbf{x}_k)$ is computed by Eq. (30).

$$\frac{\partial V(\mathbf{x}_k)}{\partial \mathbf{u}_{h,k}} = \mathbf{R}_{h,k} \mathbf{u}_{h,k} + \frac{\partial \mathbf{x}_{k+1}^T}{\partial \mathbf{u}_{h,k}} \mathbf{D}_{k+1} \mathbf{x}_{k+1} + \frac{\partial \mathbf{x}_{k+1}^T}{\partial \mathbf{u}_{h,k}} \mathbf{F}_{k+1} \quad (30)$$

$$= \mathbf{R}_{h,k} \mathbf{u}_{h,k} + \mathbf{B}_{h,k}^T \mathbf{D}_{k+1} (\mathbf{A} \mathbf{x}_k + \mathbf{B}_{h,k} \mathbf{u}_{h,k} + \mathbf{B}_{m,k} \mathbf{u}_{m,k}) + \mathbf{B}_{h,k}^T \mathbf{F}_{k+1}$$

The optimal solution $\mathbf{u}_{h,k}^*$ should satisfy $\frac{\partial V(\mathbf{x}_k)}{\partial \mathbf{u}_{h,k}} = 0$.

Hence,

$$\begin{aligned} \mathbf{u}_{h,k}^* &= -(\mathbf{R}_{h,k} + \mathbf{B}_{h,k}^T \mathbf{D}_{k+1} \mathbf{B}_{h,k})^{-1} \mathbf{B}_{h,k}^T [\mathbf{D}_{k+1} (\mathbf{A} \mathbf{x}_k \\ &+ \mathbf{B}_{m,k} \mathbf{u}_{m,k}) + \mathbf{F}_{k+1}] \end{aligned} \quad (31)$$

By defining $\mathbf{H}_{h,k}$ as Eq. (19), defining $\mathbf{K}_{h,k}$ as Eq. (20), defining $\mathbf{P}_{h,k}$ as Eq. (21), and defining $\mathbf{S}_{h,k}$ as Eq. (22), Eq. (31) could be simplified into Eq. (18).

Substituting Eq. (18) into the vehicle dynamics model in Eq. (14):

$$\mathbf{x}_{k+1} = \mathbf{N}_k \mathbf{x}_k + \mathbf{O}_k \quad (32)$$

where

$$\mathbf{O}_k = \mathbf{B}_{h,k} (\mathbf{P}_{h,k} \mathbf{u}_{m,k} + \mathbf{S}_{h,k}) + \mathbf{B}_{m,k} \mathbf{u}_{m,k} \quad (33)$$

By substituting Eqs. (18) and (32) into Eq. (29), we can derive the cost-to-go function $V(\mathbf{x}_{k-1})$ at step $k-1$. $V(\mathbf{x}_{k-1})$ should also follow second-order form as the $V(\mathbf{x}_k)$ in Eq. (29). Hence, the coefficient matrices in Eq. (29), \mathbf{D} and \mathbf{F} , could be referred iteratively as Eqs. (25) and (26).

The coefficient matrices in Eqs. (19)-(24) could be backward-iteratively computed from terminal step K to the first step. The optimal control law is received, as shown in Eq. (18). This concludes the proof. ■

It should be noted that in *Theorem 1*, the human's action $\mathbf{u}_{h,k}$ relies on the vehicle state \mathbf{x}_k and machine's command $\mathbf{u}_{m,k}$. Hence, machine controller is capable of computing commands to guide human actions as the machine's expectation.

E. Machine controller

The machine controller is developed to ensure following stability during the takeover maneuver. The controller is formulated into a GMPC problem within the Stachelberg competition framework. The human reaction function is substituted into the human-machine shared system dynamics model so that the optimization of the machine's command takes full account of human actions accordingly.

1) GMPC based controller

The machine controller could be formulated into a GMPC problem as follows. It aims at finding the optimal control series $\mathbf{u}_{m,k}|_{k=1}^{k=K}$ to enhance the following stability.

$$\min_{\mathbf{u}_{m,k}|_{k=1}^{k=K}} (J_m) = \quad (34)$$

$$\sum_{k=1}^{K-1} \Phi_{m,k}(\mathbf{x}_k, \mathbf{u}_{m,k}, \mathbf{x}_{m,k}^{ref}) + \Psi_{m,K}(\mathbf{x}_K, \mathbf{x}_{m,K}^{ref})$$

$$\text{s.t. vehicle dynamics: } f_m(\mathbf{x}_k, \mathbf{u}_{m,k}) = 0 \quad (35)$$

$$\text{State constraint: } \mathbf{x}_{min,k} \leq \mathbf{x}_k \leq \mathbf{x}_{max,k} \quad (36)$$

$$\text{Control constraint: } \mathbf{u}_{min,k} \leq \mathbf{u}_{m,k} \leq \mathbf{u}_{max,k} \quad (37)$$

where $\Phi_{m,k}$ is running cost of machine driving; $\Psi_{m,K}$ is the terminal cost of machine driving; f_m is the vehicle dynamics. The constraint on human control is not presented, since it could

be transformed into the constraints on state and machine control based on Eq. (18). The three functions $\Phi_{m,k}$, $\Psi_{m,K}$, and f_m are formulated as follows.

$$\Phi_{m,k} = \frac{1}{2} (\mathbf{x}_k - \mathbf{x}_{m,k}^{ref})^T \mathbf{Q}_{m,k} (\mathbf{x}_k - \mathbf{x}_{m,k}^{ref}) + \frac{1}{2} \mathbf{u}_{m,k}^T \mathbf{R}_{m,k} \mathbf{u}_{m,k} \quad (38)$$

$$\Psi_{m,K} = \frac{1}{2} (\mathbf{x}_K - \mathbf{x}_{m,K}^{ref})^T \mathbf{Q}_{m,K} (\mathbf{x}_K - \mathbf{x}_{m,K}^{ref}) \quad (39)$$

$$f_m = \mathbf{x}_{k+1} - \mathbf{A} \mathbf{x}_k + \mathbf{B}_{h,k} (\mathbf{K}_{h,k} \mathbf{x}_k + \mathbf{P}_{h,k} \mathbf{u}_{m,k} + \mathbf{S}_{h,k}) + \mathbf{B}_{m,k} \mathbf{u}_{m,k} + \mathbf{C} a_k^p \quad (40)$$

where $\mathbf{Q}_{m,k} = \text{diag}[q_{m,k}^v, q_{m,k}^g]$. $q_{m,k}^v$, $q_{m,k}^g$, and $\mathbf{R}_{m,k}$ are weighting factors of speed error cost, gap error cost, and control effort cost, respectively. $q_{m,k}^v$ is set as a positive value and $q_{m,k}^g$ is typically a relatively small positive value, since machine's objective is to ensure following stability at all following gaps. The vehicle dynamics model Eq. (40) is obtained from Eq. (12) after substituting human's reaction function in Eq. (18).

2) Problem transformation

The GMPC problem in Eq. (34) consists of a time-varying system dynamics model, as shown in Eq. (40). Furthermore, the non-aftereffect property is not applicable anymore, since the coefficient matrix $\mathbf{S}_{h,k}$ consists of an iterative relation of $\mathbf{u}_{m,i} \{\forall i \in [k+1, K]\}$. Hence, the GMPC problem is transformed into a Quadratic Programming (QP) problem for solving.

Defining optimization variables by containing all variables from $k=1$ to $k=K$ as follows:

$$\mathbf{U}_h \stackrel{\text{def}}{=} [\mathbf{u}_{h,1}, \mathbf{u}_{h,2}, \dots, \mathbf{u}_{h,k}, \dots, \mathbf{u}_{h,K-1}]^T \quad (41)$$

$$\mathbf{U}_m \stackrel{\text{def}}{=} [\mathbf{u}_{m,1}, \mathbf{u}_{m,2}, \dots, \mathbf{u}_{m,k}, \dots, \mathbf{u}_{m,K-1}]^T \quad (42)$$

$$\mathbf{X} \stackrel{\text{def}}{=} [\mathbf{x}_1, \mathbf{x}_2, \dots, \mathbf{x}_k, \dots, \mathbf{x}_K]^T \quad (43)$$

The human reaction function (18) in *Theorem 1* could be converted into an integrated form as Eq. (44).

$$\mathbf{U}_h = \mathcal{K}_h \mathbf{X} + (\mathcal{P}_h + \mathcal{J}_h \mathbf{S}_{h1}) \mathbf{U}_m + \mathcal{J}_h \mathbf{S}_{h2} \quad (44)$$

where

$$\mathcal{K}_h \stackrel{\text{def}}{=} \begin{bmatrix} \mathbf{K}_{h,1} & \mathbf{0} & \dots & \mathbf{0} & \mathbf{0} \\ \mathbf{0} & \mathbf{K}_{h,2} & \dots & \mathbf{0} & \mathbf{0} \\ \vdots & \vdots & \ddots & \mathbf{0} & \vdots \\ \mathbf{0} & \mathbf{0} & \dots & \mathbf{K}_{h,K-1} & \mathbf{0} \end{bmatrix} \quad (45)$$

$$\mathcal{P}_h \stackrel{\text{def}}{=} \begin{bmatrix} \mathbf{P}_{h,1} & \mathbf{0} & \dots & \mathbf{0} \\ \mathbf{0} & \mathbf{P}_{h,2} & \dots & \mathbf{0} \\ \vdots & \vdots & \ddots & \mathbf{0} \\ \mathbf{0} & \mathbf{0} & \dots & \mathbf{P}_{h,K-1} \end{bmatrix} \quad (46)$$

$$\mathcal{J}_h \stackrel{\text{def}}{=} \begin{bmatrix} -\mathbf{H}_{h,1} \mathbf{B}_{h,1}^T & \mathbf{0} & \dots & \mathbf{0} \\ \mathbf{0} & -\mathbf{H}_{h,2} \mathbf{B}_{h,2}^T & \dots & \mathbf{0} \\ \vdots & \vdots & \ddots & \mathbf{0} \\ \mathbf{0} & \mathbf{0} & \dots & -\mathbf{H}_{h,K-1} \mathbf{B}_{h,K-1}^T \end{bmatrix} \quad (47)$$

$$\mathcal{S}_{h1} \stackrel{\text{def}}{=} \begin{bmatrix} \mathbf{0}(\mathbf{M}_{h,2} + \mathbf{N}_2^T) \mathbf{D}_3 \mathbf{B}_{m,2} \cdots \prod_{w=2}^c ((\mathbf{M}_{h,w} + \mathbf{N}_w^T)) \mathbf{D}_{c+1} \mathbf{B}_{m,c} \cdots \prod_{w=2}^{K-1} (\mathbf{M}_{h,w} + \mathbf{N}_w^T) \mathbf{D}_K \mathbf{B}_{m,K-1} \\ \mathbf{0} \quad \mathbf{0} \quad \vdots \quad \vdots \quad \cdots \quad \vdots \\ \mathbf{0} \quad \mathbf{0} \quad \vdots \prod_{w=r+1}^c ((\mathbf{M}_{h,w} + \mathbf{N}_w^T)) \mathbf{D}_{c+1} \mathbf{B}_{m,c} \cdots \prod_{w=r+1}^{K-1} ((\mathbf{M}_{h,w} + \mathbf{N}_w^T)) \mathbf{D}_K \mathbf{B}_{m,K-1} \\ \vdots \quad \vdots \quad \vdots \quad \vdots \quad \cdots \quad \vdots \\ \mathbf{0} \quad \mathbf{0} \quad \mathbf{0} \quad \mathbf{0} \quad \mathbf{0} \quad (\mathbf{M}_{h,K-1} + \mathbf{N}_{K-1}^T) \mathbf{D}_K \mathbf{B}_{m,K-1} \\ \mathbf{0} \quad \mathbf{0} \quad \mathbf{0} \quad \mathbf{0} \quad \mathbf{0} \quad \mathbf{0} \end{bmatrix} \quad (48)$$

$$\mathcal{S}_{h2} \stackrel{\text{def}}{=} \begin{bmatrix} -\sum_{j=1}^{K-1} \left(\prod_{w=2}^j ((\mathbf{M}_{h,w} + \mathbf{N}_w^T)) \mathbf{Q}_{h,j+1} \mathbf{x}_{h,j+1}^{\text{ref}} \right) \\ \vdots \\ -\sum_{j=r}^{K-1} \left(\prod_{w=r+1}^j ((\mathbf{M}_{h,w} + \mathbf{N}_w^T)) \mathbf{Q}_{h,j+1} \mathbf{x}_{h,j+1}^{\text{ref}} \right) \\ \vdots \\ -\mathbf{Q}_{h,K} \mathbf{x}_{h,K}^{\text{ref}} \end{bmatrix} \quad (49)$$

Finally, the GMPC problem in Eq. (34) could be transformed into a QP form as follows.

$$\min_{\mathbf{U}_m} (J_m) = \frac{1}{2} \begin{pmatrix} \mathbf{X} \\ \mathbf{U}_m \end{pmatrix}^T \mathbb{D}_m \begin{pmatrix} \mathbf{X} \\ \mathbf{U}_m \end{pmatrix} + \begin{pmatrix} \mathbf{X} \\ \mathbf{U}_m \end{pmatrix}^T \mathbb{F}_m \quad (50)$$

s.t.

$$(\mathbf{I} - \mathcal{A}_m - \mathcal{B}_h \mathcal{K}_h - \mathcal{B}_h \mathcal{P}_h - \mathcal{B}_h \mathcal{T}_h \mathcal{S}_{h1} - \mathcal{B}_m) \begin{pmatrix} \mathbf{X} \\ \mathbf{U}_m \end{pmatrix} = \quad (51)$$

$$\mathcal{B}_h \mathcal{T}_h \mathcal{S}_{h2} + \mathcal{C}_m$$

where

$$\mathbf{X}_m^{\text{ref}} \stackrel{\text{def}}{=} [\mathbf{x}_{m,1}^{\text{ref}}, \mathbf{x}_{m,2}^{\text{ref}}, \dots, \mathbf{x}_{m,k'}^{\text{ref}}, \dots, \mathbf{x}_{m,K}^{\text{ref}}]^T \quad (52)$$

$$\mathcal{Q}_m \stackrel{\text{def}}{=} \begin{bmatrix} \mathbf{Q}_{m,1} & \mathbf{0} & \cdots & \mathbf{0} \\ \mathbf{0} & \mathbf{Q}_{m,2} & \cdots & \mathbf{0} \\ \vdots & \vdots & \ddots & \vdots \\ \mathbf{0} & \mathbf{0} & \cdots & \mathbf{Q}_{m,K} \end{bmatrix} \quad (53)$$

$$\mathcal{R}_m \stackrel{\text{def}}{=} \begin{bmatrix} \mathbf{R}_{m,1} & \mathbf{0} & \cdots & \mathbf{0} \\ \mathbf{0} & \mathbf{R}_{m,2} & \cdots & \mathbf{0} \\ \vdots & \vdots & \ddots & \vdots \\ \mathbf{0} & \mathbf{0} & \cdots & \mathbf{R}_{m,K-1} \end{bmatrix} \quad (54)$$

$$\mathcal{A}_m \stackrel{\text{def}}{=} \begin{bmatrix} \mathbf{0} & \mathbf{0} & \cdots & \mathbf{0} & \mathbf{0} \\ \mathbf{A} & \mathbf{0} & \cdots & \mathbf{0} & \mathbf{0} \\ \mathbf{0} & \mathbf{A} & \ddots & \mathbf{0} & \mathbf{0} \\ \vdots & \vdots & \ddots & \vdots & \vdots \\ \mathbf{0} & \mathbf{0} & \cdots & \mathbf{A} & \mathbf{0} \end{bmatrix} \quad (55)$$

$$\mathcal{B}_h \stackrel{\text{def}}{=} \begin{bmatrix} \mathbf{0} & \mathbf{0} & \cdots & \mathbf{0} \\ \mathbf{B}_{h,1} & \mathbf{0} & \cdots & \mathbf{0} \\ \mathbf{0} & \mathbf{B}_{h,2} & \ddots & \mathbf{0} \\ \vdots & \vdots & \ddots & \vdots \\ \mathbf{0} & \mathbf{0} & \cdots & \mathbf{B}_{h,K-1} \end{bmatrix} \quad (56)$$

$$\mathcal{B}_m \stackrel{\text{def}}{=} \begin{bmatrix} \mathbf{0} & \mathbf{0} & \cdots & \mathbf{0} \\ \mathbf{B}_{m,1} & \mathbf{0} & \cdots & \mathbf{0} \\ \mathbf{0} & \mathbf{B}_{m,2} & \ddots & \mathbf{0} \\ \vdots & \vdots & \ddots & \vdots \\ \mathbf{0} & \mathbf{0} & \cdots & \mathbf{B}_{m,K-1} \end{bmatrix} \quad (57)$$

$$\mathcal{C}_m \stackrel{\text{def}}{=} \begin{bmatrix} \mathbf{x}_1 \\ \mathbf{0} \\ \vdots \\ \mathbf{0} \end{bmatrix} + \begin{bmatrix} \mathbf{C} & \mathbf{0} & \cdots & \mathbf{0} \\ \mathbf{0} & \mathbf{C} & \ddots & \mathbf{0} \\ \vdots & \vdots & \ddots & \vdots \\ \mathbf{0} & \mathbf{0} & \cdots & \mathbf{C} \end{bmatrix} \mathbf{a}^p \quad (58)$$

$$\mathbb{D}_m \stackrel{\text{def}}{=} \begin{bmatrix} \mathcal{Q}_m & \mathbf{0} \\ \mathbf{0} & \mathcal{R}_m \end{bmatrix} \quad (59)$$

$$\mathbb{F}_m \stackrel{\text{def}}{=} \begin{bmatrix} -\mathcal{Q}_m \mathbf{X}_m^{\text{ref}} \\ \mathbf{0} \end{bmatrix} \quad (60)$$

where $\mathbf{a}^p \stackrel{\text{def}}{=} [a_1^p, a_2^p, \dots, a_{K-1}^p]^T$.

3) Optimal solution

The QP problem (50) could be solved by the iterative Lagrange multiplier method [31].

Theorem 2: The optimal solution of problem (50) is as follows.

$$\begin{pmatrix} \mathbf{X} \\ \mathbf{U}_m \\ \boldsymbol{\lambda}^T \end{pmatrix} = \begin{bmatrix} \mathbb{D}_m & \mathbb{W}_m^T \\ \mathbb{W}_m & \mathbf{0} \end{bmatrix}^{-1} \begin{bmatrix} -\mathbb{F}_m \\ \mathbb{Z}_m \end{bmatrix} \quad (61)$$

$$\mathbb{W}_m \stackrel{\text{def}}{=} (\mathbf{I} - \mathcal{A}_m - \mathcal{B}_h \mathcal{K}_h - \mathcal{B}_h \mathcal{P}_h - \mathcal{B}_h \mathcal{T}_h \mathcal{S}_{h1} - \mathcal{B}_m) \quad (62)$$

$$\mathbb{Z}_m \stackrel{\text{def}}{=} \mathcal{B}_h \mathcal{T}_h \mathcal{S}_{h2} + \mathcal{C}_m \quad (63)$$

where $\boldsymbol{\lambda}$ is the Lagrange multiplier.

Proof:

Introducing Lagrange multiplier $\boldsymbol{\lambda}$ and defining Lagrange function \mathbb{L} as:

$$\mathbb{L} \stackrel{\text{def}}{=} \frac{1}{2} \begin{pmatrix} \mathbf{X} \\ \mathbf{U}_m \end{pmatrix}^T \mathbb{D}_m \begin{pmatrix} \mathbf{X} \\ \mathbf{U}_m \end{pmatrix} + \begin{pmatrix} \mathbf{X} \\ \mathbf{U}_m \end{pmatrix}^T \mathbb{F}_m + \boldsymbol{\lambda} \left[\mathbb{W}_m \begin{pmatrix} \mathbf{X} \\ \mathbf{U}_m \end{pmatrix} - \mathbb{Z}_m \right] \quad (64)$$

The optimal solution $\begin{pmatrix} \mathbf{X}^* \\ \mathbf{U}_m^* \end{pmatrix}$ is obtained by computing the derivative of \mathbb{L} :

$$\frac{\partial \mathbb{L}}{\partial \begin{pmatrix} \mathbf{X} \\ \mathbf{U}_m \end{pmatrix}} = \mathbb{D}_m \begin{pmatrix} \mathbf{X} \\ \mathbf{U}_m \end{pmatrix} + \mathbb{F}_m + \mathbb{W}_m^T \boldsymbol{\lambda}^T = \mathbf{0} \quad (65)$$

$$\frac{\partial \mathbb{L}}{\partial \boldsymbol{\lambda}} = \mathbb{W}_m \begin{pmatrix} \mathbf{X} \\ \mathbf{U}_m \end{pmatrix} - \mathbb{Z}_m = \mathbf{0} \quad (66)$$

Solving the Eqs. (65) and (66), the optimal solution could be computed into Eq. (61). This concludes the proof. ■

III. EVALUATION

Simulation is conducted on the Matlab platform. The proposed human-machine shared CACC controller is evaluated from the following perspectives: i) the function of smooth takeover; ii) platoon sting stability; iii) perceived safety in regard to traffic oscillations; iv) actual safety in regard to hard brakes; v) influence on upstream traffic.

A. Controller types

There are two types of CACC controllers to be tested:

• **The proposed human-machine shared CACC controller:** This controller is capable of allocating control authority between human and machine. Different allocation

factors could be selected. The machine could generate proactive control commands with the consideration of the preceding vehicle's future commands.

- **Baseline human driver:** Human drivers directly take over the control authority from the machine. Human actions are delayed without acquiring the preceding vehicle's future actions.

B. Test scenarios

The proposed CACC controller is tested on the highway environment. The CACC platoon is following a preceding HV. CACC takeover is needed from time to time. For example, human drivers may be asked to take over the CACC platoon in order to get off the highway. Three cases are designed as follows:

- **Case 1:** The preceding HV is cruising at a constant speed of 10 m/s. The proposed CACC controller adopts three types of takeover strategies, i) including linear gradient from machine to human, ii) constant allocation (30% of authority is given to human), and iii) human's direct takeover (100% of authority is given to human).
- **Case 2:** The preceding HV imposes a speed oscillation influence on the CACC platoon. The preceding HV's speed oscillation follows a sinusoidal function.
- **Case 3:** The preceding HV conducts a hard brake.

C. Measures of effectiveness

Measures of Effectiveness (MOEs) adopted are as follows.

- **Function validation:** The function of smoothly taking over a CACC system is validated by trajectories of the following gap, speed difference, and acceleration. This MOE is tested in the scenario of Case 1.
- **String stability:** This MOE is evaluated by vehicles' following gap trajectories and gap range. Moreover, the ODD to ensure string stability is quantified by the oscillation propagation rate within the platoon $\Theta_{n,i,i-1}$, calculated as follows. This MOE is tested in the scenario of Case 2.

$$\Theta_{n,i,i-1} \stackrel{\text{def}}{=} E \left(\frac{\|g^i\|_2}{\|g^{i-1}\|_2} \right), \forall i \in [2, n] \quad (67)$$

where n is the number of CAVs within a platoon; $\Theta_{n,i,i-1}$ is the oscillation propagation rate between the CAV i and its preceding CAV $i-1$

- **Perceived safety:** This MOE is evaluated by the vehicles' acceleration range [32]. It is tested in the scenario of Case 2.
- **Actual safety:** This MOE is evaluated by vehicles' following gap trajectories and gap range. This MOE is tested in the scenario of Case 3.
- **Traffic influence:** CACC's influence on upstream traffic is evaluated by vehicle trajectories and quantified by speed oscillation ranges. The influence range is identified. This MOE is tested in the scenario of Case 2.

D. Results

Results demonstrate that the proposed CACC takeover controller is capable of i) dynamically allocating control authority between machine and human to ensure a smooth takeover; ii) ensuring string stability when human's control authority is under 32.7%; iii) enhancing perceived safety and actual safety by machine's intervention; iv) reducing influence on upstream traffic.

1) Function validation

The function of smoothly taking over a CACC system is demonstrated by following gap and speed difference trajectories, as shown in Fig. 3. Three types of takeover strategies are tested, including human's direct takeover (Fig. 3-I), 30% of authority to human (Fig. 3-II), and a linear gradient of authority (Fig. 3-III). Results show that the involvement of the machine would obtain a smoother CACC takeover maneuver, as illustrated in Fig. 3 (II) and (III). Compared to the human driver's direct takeover, the proposed method reduces speed oscillation magnitude by extending the duration of the takeover. It indicates that the proposed controller is good at making a tradeoff between space and time.

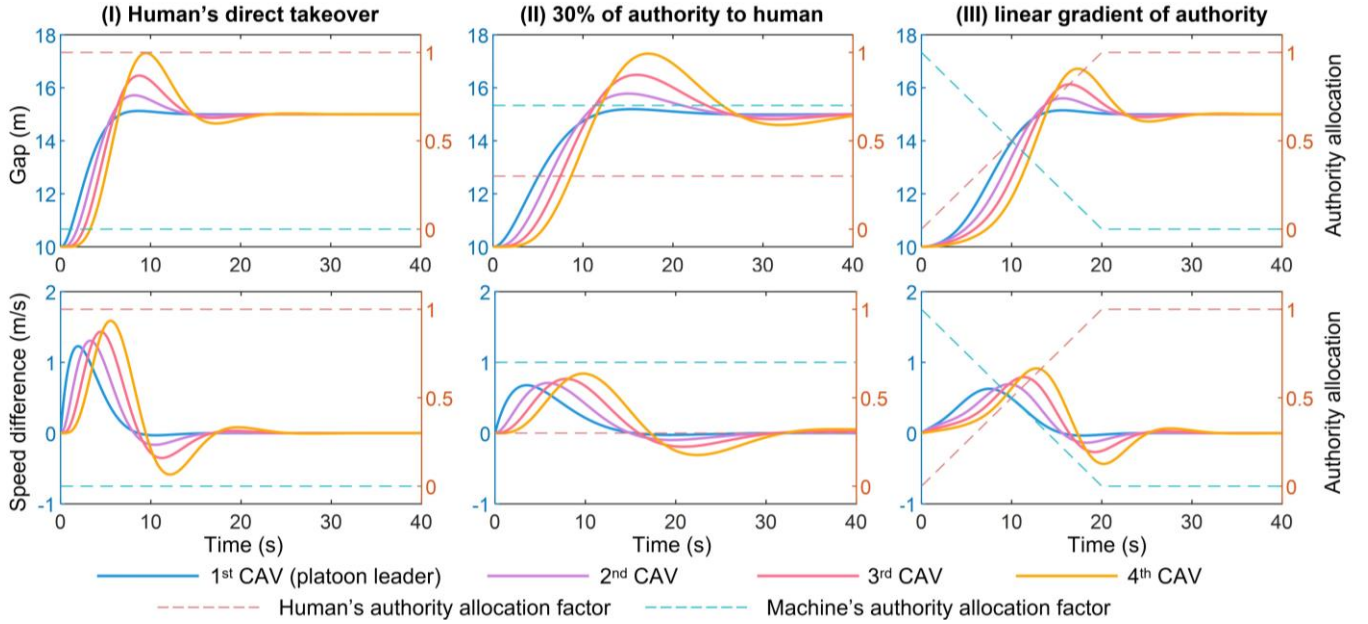


Fig. 3. Trajectories of a CACC takeover maneuver for the proposed method.

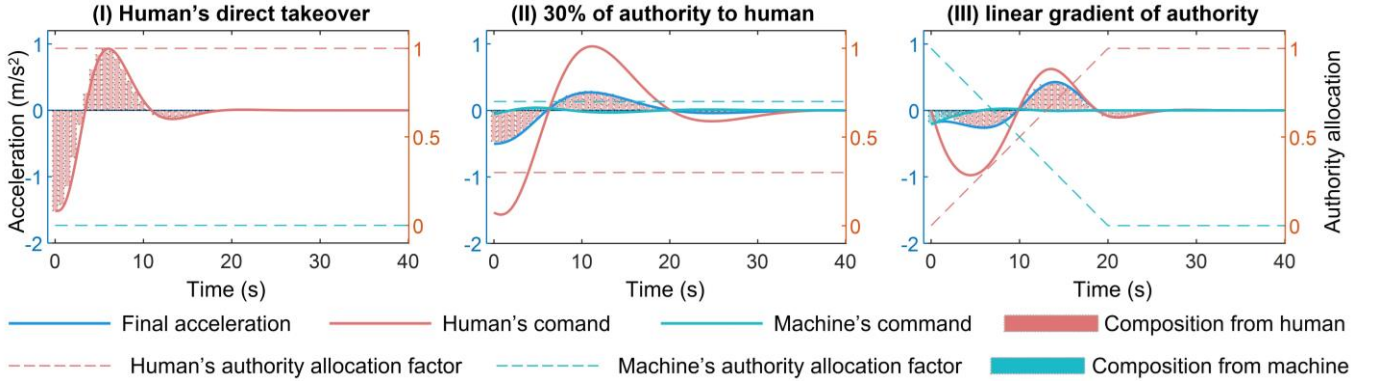


Fig. 4. Human-machine shared control authority allocation process.

The function of human-machine shared control is verified by vehicles' command trajectories. The third CAV's acceleration and its compositions from human and machine are selected for illustrations, as shown in Fig. 4. Compared to human's direct takeover in Fig. 4 (I), allocating 70% of authority to machine (Fig. 4-II) could avoid hard brakes at the beginning of takeover. Furthermore, a linear gradient authority allocation strategy can better smooth the takeover trajectory, as shown in Fig. 4 (III). In this case, with the decrease of the machine's authority and increase of human's authority, the vehicle's final acceleration command exhibits an increasing dominance by the human driver. It enables CACC to gradually hand over the control authority from machine to human. At the beginning of the takeover, the machine has greater control authority. Final acceleration has a larger composition from the machine, as illustrated by the green bar in Fig. 4. This avoids human stress behaving at the beginning of the takeover, where there is no more hard braking as shown by the red solid line in Fig. 4 (III). When the human driver gets into its stride typically within 10 seconds, more authority would be allocated to human to gradually accomplish the CACC takeover maneuver.

2) String stability

A sensitivity analysis is conducted on string stability in terms of various authority allocation factors for the proposed CACC controller. The following gap trajectories are illustrated in Fig. 5. It shows that the following gap oscillations are reduced when propagating along the platoon string, when the CACC platoon is entirely controlled by machine, as shown in Fig. 5 (I), or 20% of control authorities are allocated to human, as shown in Fig. 5 (II). When more than 40% of control authorities are given to human, as shown in Fig. 5 (III) and (IV), the following gap oscillations are amplified by the following vehicles. In these cases, string stability is not ensured.

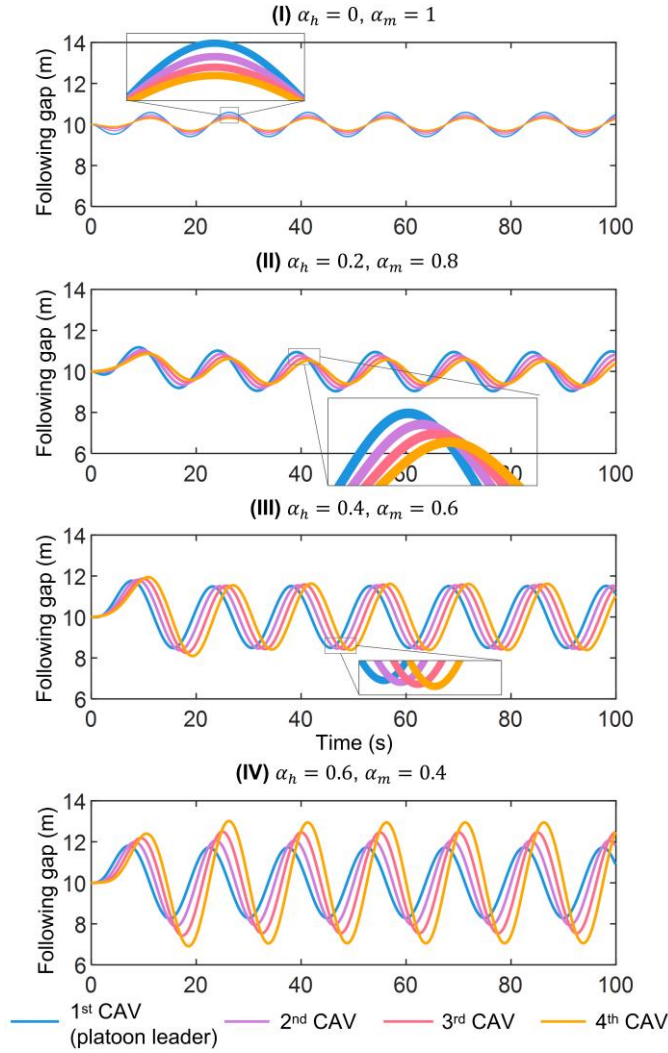


Fig. 5. Sensitivity analysis on following gap trajectories in terms of authority allocation factors.

The ODD of ensuring CACC's string stability is quantified in regard to various control authority allocation factors, as shown in Fig. 6. Results show that to ensure string stability, the proportion of human control authority shall be less than 32.7%. In this setting, the following gap range would be reduced along the CACC string, as illustrated in Fig. 6 (I), and the oscillation propagation rate is less than 1, as illustrated in Fig. 6 (II). Hence, within the ODD of human control authority of less than 32.7%, the proposed controller is capable of ensuring string stability and avoiding disturbances being amplified when propagating along platoon strings.

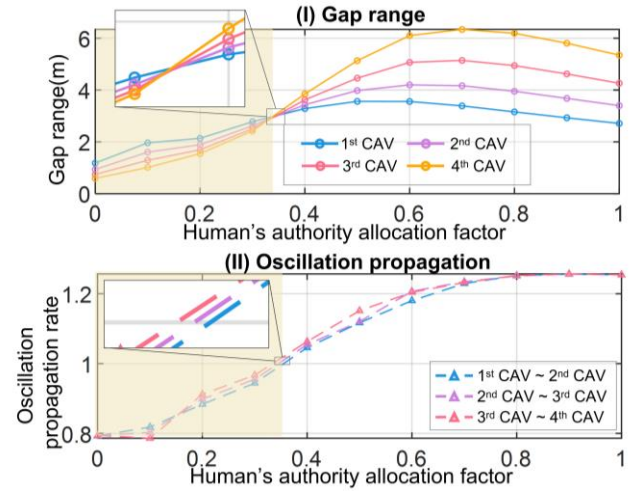


Fig. 6. ODD of ensuring string stability.

3) Perceived safety

The perceived safety is evaluated by the acceleration range in three different authority allocation factors, as illustrated in Fig. 7. Results show that 30% of the machine's control authority (Fig. 7-II) would enhance perceived safety by 53.23%, compared to fully human's control (Fig. 7-IV). When string stability is ensured, as shown in Fig. 7 (I) and (II), the acceleration range is reduced along the platoon string. This indicates that all CAVs would be enabled with perceived safety, no matter how long the CACC platoon is. However, with the decrease of the machine's authority (from Fig. 7-I to IV), the acceleration range of followers increases. Under full human's control ($\alpha_h = 1$), as shown in Fig. 7 (IV), all following CAVs have greater acceleration range compared to the preceding HV. Moreover, the acceleration range is amplified along the platoon string. It indicates that perceived safety would be reduced along platoon string under the control of human drivers.

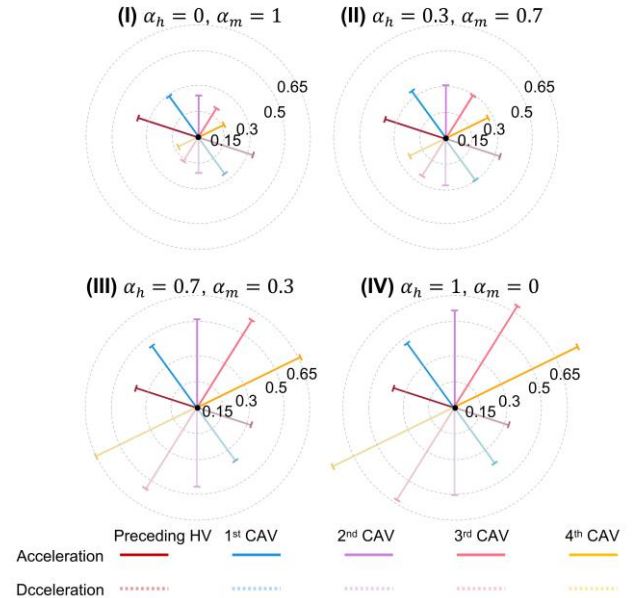


Fig. 7. Acceleration range in various authority allocation factors.

4) Actual safety

A sensitivity analysis is conducted for actual safety evaluation regarding authority allocation factors. In the test scenario, the leading HV conducts a hard brake. The vehicles' following gap distributions and minimum following gap are illustrated in Fig. 8. Results demonstrate that the proposed controller is capable of ensuring actual safety when the human control authority is less than 0.4. In these cases, the minimum following gap is greater than the safety threshold, as illustrated in Fig. 8. However, when most of the control authorities are given to humans, collisions cannot be avoided. Hence, it is

advised to restrict human control authority under 0.4 under the following gap so that human drivers could have enough reaction time. Furthermore, it could be noted that following gap oscillations increase with the increase of human's control authority, as shown in Fig. 8. When a human's control authority is less than 0.4, the minimum following gap would not increase along the platoon string. However, when human control authority increases, following gap oscillations are enhanced since the range of outliers significantly increases along the platoon string. This confirms the sting stability analysis in Fig. 6.

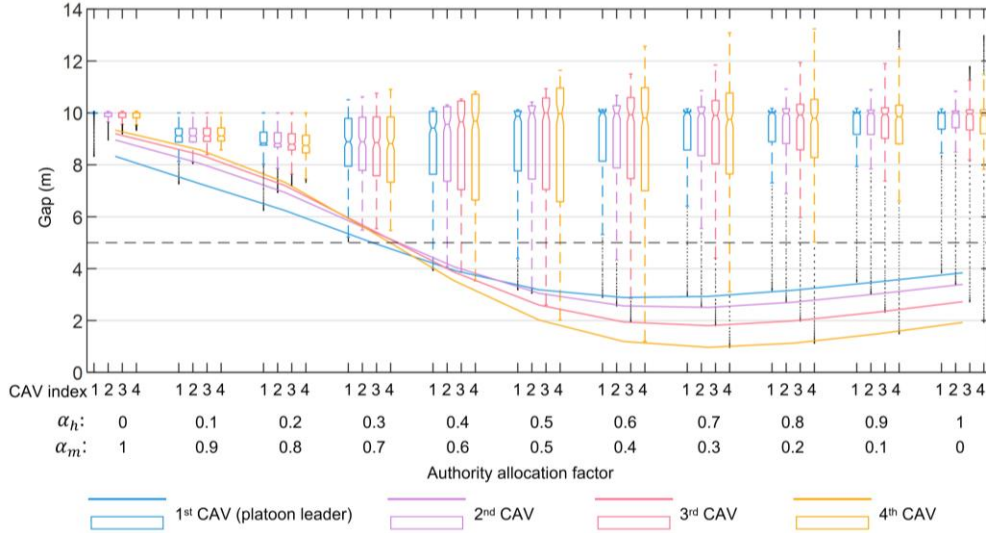


Fig. 8. Following gap distributions when leading HV conducts a hard brake.

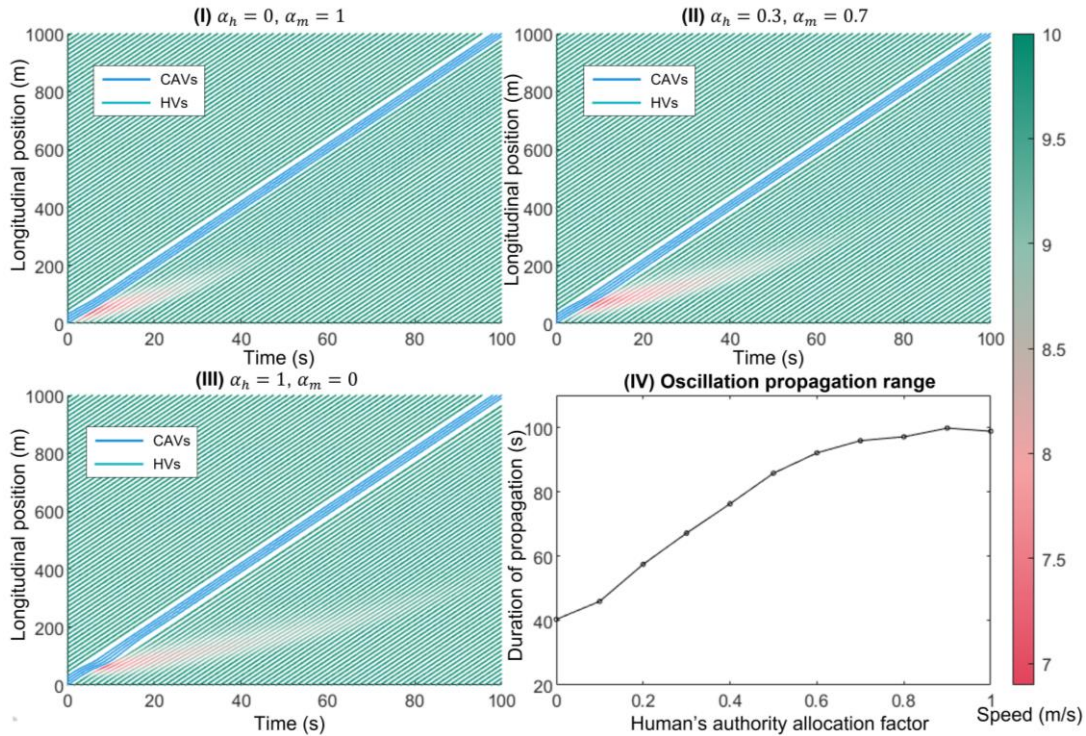


Fig. 9. Traffic influence evaluation and qualification.

5) Traffic influence

The proposed controller is verified to reduce traffic

oscillations compared to human direct takeover. The human and machine shared control scheme reduces traffic oscillation

propagation, as illustrated in Fig. 9 (II), compared to entirely human control authority Fig. 9 (III). Moreover, when the machine is given greater control authority, there will be fewer traffic oscillations, as shown in Fig. 9 (I). The traffic influence range is quantified by the duration of traffic oscillation propagation, as illustrated in Fig. 9 (IV). It shows that the proposed controller is capable of reducing 60% traffic influence, by reducing the duration of traffic oscillation propagation. Moreover, traffic influence is reduced with the increase of human control authority. When the CACC platoon is fully controlled by the machine, traffic oscillation would propagate for only 40 seconds. However, when the platoon is fully controlled by humans, traffic oscillation would propagate for 100 seconds.

IV. CONCLUSIONS

This research introduces a Cooperative Adaptive Cruise Control (CACC) takeover controller based on a human-machine shared control approach, formulated as a Stackelberg competition between the machine and the human. The machine controller leads human actions by incorporating the human reaction function into the system dynamics. The proposed controller achieves the following objectives: i) enables a smooth takeover maneuver of CACC; ii) ensures string stability within a specific Operational Design Domain (ODD); iii) enhances perceived and actual safety; iv) reduces traffic oscillation propagation. Simulation results demonstrate that:

- The proposed controller can dynamically allocate control authority between the machine and the human to ensure a smooth takeover.
- It ensures string stability within a specific ODD when human control authority is under 32.7%.
- Machine interventions enhance perceived safety by at least 53.23%.
- The controller ensures actual safety when string stability is maintained.
- It reduces the influence on upstream traffic by up to 60%.
- Human control authority should be set below 0.3 until the following gap is sufficiently large.

This research primarily focuses on developing the human-machine shared CACC takeover controller. Therefore, it infers the human reaction function without considering individual driving preferences. Future studies and implementations could incorporate a human-driving style identification module to further enhance CACC takeover performance.

REFERENCES

- [1] M. Zhou, X. Qu, and S. Jin, "On the impact of cooperative autonomous vehicles in improving freeway merging: a modified intelligent driver model-based approach," *IEEE Transactions on Intelligent Transportation Systems*, vol. 18, no. 6, pp. 1422-1428, 2017.
- [2] I. G. Jin and G. Orosz, "Connected cruise control among human-driven vehicles: Experiment-based parameter estimation and optimal control design," *Transportation research part C: emerging technologies*, vol. 95, pp. 445-459, 2018.
- [3] J. Hu, H. Wang, X. Li, and X. Li, "Modelling merging behaviour joining a cooperative adaptive cruise control platoon," *IET Intelligent Transport Systems*, 2020.
- [4] A. Vahidi and A. Sciarretta, "Energy saving potentials of connected and automated vehicles," *Transportation Research Part C: Emerging Technologies*, 2018.
- [5] B. B. Park, K. Malakorn, and J. Lee, "Quantifying benefits of cooperative adaptive cruise control towards sustainable transportation system," 2011.
- [6] X. Hua, W. Yu, Y. Xiang, D. Zhao, and W. Wang, "Impact Analysis of Driver Takeover Under a Connected Environment: A Study of the External Effects on Vehicle Conversions," *Transportation Research Record*, p. 03611981231172965, 2023.
- [7] S. E. Shladover, D. Su, and X.-Y. Lu, "Impacts of cooperative adaptive cruise control on freeway traffic flow," *Transportation Research Record*, vol. 2324, no. 1, pp. 63-70, 2012.
- [8] C. Gasne, L. Paire-Ficout, S. Bordel, S. Lafont, and M. Ranchet, "Takeover performance of older drivers in automated driving: a review," *Transportation research part F: traffic psychology and behaviour*, vol. 87, pp. 347-364, 2022.
- [9] N. Merat, A. H. Jamson, F. C. Lai, M. Daly, and O. M. Carsten, "Transition to manual: Driver behaviour when resuming control from a highly automated vehicle," *Transportation research part F: traffic psychology and behaviour*, vol. 27, pp. 274-282, 2014.
- [10] J. Hu, H. Wang, X. Li, and X. Li, "Modelling merging behaviour joining a cooperative adaptive cruise control platoon," *IET Intelligent Transport Systems*, vol. 14, no. 7, pp. 693-701, 2020.
- [11] H. Wang and J. Hu, "A Cooperative Lane Change Controller with a Time-Varying Desired State Function," in *2022 IEEE 25th International Conference on Intelligent Transportation Systems (ITSC)*, 2022: IEEE, pp. 1837-1841.
- [12] H. Wang, J. Lai, X. Zhang, Y. Zhou, S. Li, and J. Hu, "Make space to change lane: A cooperative adaptive cruise control lane change controller," *Transportation research part C: emerging technologies*, vol. 143, p. 103847, 2022.
- [13] H. Wang, X. Li, X. Zhang, J. Hu, X. Yan, and Y. Feng, "Cut Through Traffic Like a Snake: Cooperative Adaptive Cruise Control with Successive Platoon Lane Change Capability," *Journal of Intelligent Transportation Systems*, 2022.
- [14] X. Tan, B. Liu, J. Chen, and Z. Jiang, "Observer-Based Resilient Control of CACC Vehicle Platoon Against DoS Attack," *Automotive Innovation*, vol. 6, no. 2, pp. 176-189, 2023.
- [15] K. Okada, K. Sonoda, and T. Wada, "Transferring from automated to manual driving when traversing a curve via haptic shared control," *IEEE Transactions on Intelligent Vehicles*, vol. 6, no. 2, pp. 266-275, 2020.
- [16] T. Saito, T. Wada, and K. Sonoda, "Control authority transfer method for automated-to-manual driving via a shared authority mode," *IEEE Transactions on Intelligent Vehicles*, vol. 3, no. 2, pp. 198-207, 2018.
- [17] Z. Zhang, C. Wang, W. Zhao, C. Xu, and G. Chen, "Driving authority allocation strategy based on driving authority real-time allocation domain," *IEEE Transactions on Intelligent Transportation Systems*, vol. 23, no. 7, pp. 8528-8543, 2021.
- [18] A. Rangesh, N. Deo, R. Greer, P. Gunaratne, and M. M. Trivedi, "Autonomous vehicles that alert humans to take-over controls: Modeling with real-world data," in *2021 IEEE International Intelligent Transportation Systems Conference (ITSC)*, 2021: IEEE, pp. 231-236.
- [19] Z. Fang, J. Wang, Z. Wang, J. Chen, G. Yin, and H. Zhang, "Human-machine shared control for path following considering driver fatigue characteristics," *IEEE Transactions on Intelligent Transportation Systems*, 2024.
- [20] M. Li, C. Jiang, X. Song, and H. Cao, "Parameter effects of the potential-field-driven model predictive controller for shared control," *Automotive Innovation*, vol. 6, no. 1, pp. 48-61, 2023.
- [21] R. Li, Y. Li, S. E. Li, C. Zhang, E. Burdet, and B. Cheng, "Indirect shared control for cooperative driving between driver and automation in steer-by-wire vehicles," *IEEE Transactions on Intelligent Transportation Systems*, vol. 22, no. 12, pp. 7826-7836, 2020.
- [22] K. O. Koerten, D. A. Abbink, and A. Zgonnikov, "Haptic Shared Control for Dissipating Phantom Traffic Jams," *IEEE Transactions on Human-Machine Systems*, 2024.
- [23] S. Musić and S. Hirche, "Haptic shared control for human-robot collaboration: A game-theoretical approach," *IFAC-PapersOnLine*, vol. 53, no. 2, pp. 10216-10222, 2020.
- [24] W. Li, Q. Li, S. E. Li, R. Li, Y. Ren, and W. Wang, "Indirect Shared Control Through Non-Zero Sum Differential Game for Cooperative Automated Driving," *IEEE Transactions on Intelligent Transportation Systems*, 2022.
- [25] X. Zhao *et al.*, "Indirect shared control strategy for human-machine cooperative driving on hazardous curvy roads," *IEEE Transactions on*

- Intelligent Vehicles*, vol. 8, no. 3, pp. 2257-2270, 2023.
- [26] G. Lucente, R. Dariani, J. Schindler, and M. Ortgieste, "A Bayesian Approach with Prior Mixed Strategy Nash Equilibrium for Vehicle Intention Prediction," *Automotive Innovation*, vol. 6, no. 3, pp. 425-437, 2023.
 - [27] G. J. Naus, R. P. Vugts, J. Ploeg, M. J. van De Molengraft, and M. Steinbuch, "String-stable CACC design and experimental validation: A frequency-domain approach," *IEEE Transactions on vehicular technology*, vol. 59, no. 9, pp. 4268-4279, 2010.
 - [28] Y. Zhou, M. Wang, and S. Ahn, "Distributed model predictive control approach for cooperative car-following with guaranteed local and string stability," *Transportation research part B: methodological*, vol. 128, pp. 69-86, 2019.
 - [29] H. Wang, J. Hu, Y. Feng, and X. Li, "Optimal control-based highway pilot motion planner with stochastic traffic consideration," *IEEE Intell. Transp. Syst. Mag.*, 2022.
 - [30] H. Guo, Y. Ji, T. Qu, and H. Chen, "Understanding and modeling the human driver behavior based on MPC," *IFAC Proceedings Volumes*, vol. 46, no. 21, pp. 133-138, 2013.
 - [31] K. Ito and K. Kunisch, *Lagrange multiplier approach to variational problems and applications*. SIAM, 2008.
 - [32] M. Frigo and S. G. Johnson, "FFTW: an adaptive software architecture for the FFT," in *Proceedings of the 1998 IEEE International Conference on Acoustics, Speech and Signal Processing, ICASSP '98 (Cat. No.98CH36181)*, 15-15 May 1998 1998, vol. 3, pp. 1381-1384 vol.3, doi: 10.1109/ICASSP.1998.681704.